UNIVERSIDAD SAN FRANCISCO DE QUITO USFQ

Colegio de Ciencias e Ingenierías

Development of a Film Based on Oxidized *Ipomea Batatas L.* Starch with Protein Encapsulation for Potential Skin Tissue Engineering Applications
Proyecto de investigación

Daniela Alejandra Viteri Narváez

Ingeniería Química

Trabajo de titulación de pregrado presentado como requisito

para la obtención del título de Ingeniera Química

Quito, 18 de mayo de 2018

UNIVERSIDAD SAN FRANCISCO DE QUITO USFQ

COLEGIO DE CIENCIAS E INGENIERÍAS

HOJA DE CALIFICACIÓN DE TRABAJO DE TITULACIÓN

Development of a Film Based on Oxidized *Ipomea Batatas L.* Starch with Protein Encapsulation for Potential Skin Tissue Engineering Applications

Daniela Alejandra Viteri Narváez

Calificación:

Nombre del profesor, Título académico   José Francisco Álvarez Barreto, Ph.D.

Firma del profesor   ---

Quito, 18 de mayo de 2018

© Derechos de Autor

Por medio del presente documento certifico que he leído todas las Políticas y Manuales de la Universidad San Francisco de Quito USFQ, incluyendo la Política de Propiedad Intelectual USFQ, y estoy de acuerdo con su contenido, por lo que los derechos de propiedad intelectual del presente trabajo quedan sujetos a lo dispuesto en esas Políticas.

Asimismo, autorizo a la USFQ para que realice la digitalización y publicación de este trabajo en el repositorio virtual, de conformidad a lo dispuesto en el Art. 144 de la Ley Orgánica de Educación Superior.

Firma del estudiante:

Nombres y Apellidos: Daniela Alejandra Viteri Narváez

Código de estudiante: 00117985

C. I.:   1721741211

Lugar, Fecha   Quito, 18 de mayo de 2018

Resumen

Los almidones han sido utilizados ampliamente como biopolímeros en la ingeniería de tejidos debido a sus propiedades únicas, su biocompatibilidad y biodegradabilidad, sin embargo, el almidón de camote no ha sido investigado en este campo. Por estas razones se plantea realizar películas poliméricas a base de almidón de camote oxidado con PVA y glicerina para encapsular un extracto proteico de la gelatina de Wharton. Se utilizó un diseño experimental utilizando BSA como proteína modelo para analizar las propiedades de los apósitos. Tanto los almidones como las películas poliméricas fueron caracterizadas por espectroscopías infrarrojas por transformadas de Fourier (FTIR), en donde se observan interacciones de los grupos carbonilo de los almidones oxidados con los grupos amino de las proteínas en la posible formación de bases de Schiff, así como se confirman las oxidaciones de los almidones en base a las vibraciones de los grupos aldehídos carbonilos. La microscopía electrónica de barrido (SEM), se utilizó para las superficies de los films y la microscopía óptica para observar la morfología del almidón nativo. Se utilizaron métodos analíticos para determinar la mejor composición de las películas poliméricas basándose en el método de superficie de respuesta en donde las variables de salida fueron el hinchamiento y liberación en el equilibrio y el grosor de las películas, y las variables de entrada fueron el volumen de la mezcla polimérica, el grado de oxidación del almidón y la cantidad de almidón nativo, manteniendo constante el porcentaje de PVA (2%w/v), glicerina (2% v/v) y BSA (5%w/w del total del almidón). En todas las formulaciones se aprecian superficies uniformes rugosas en las imágenes generadas por el SEM, se puede apreciar de igual forma que a medida que incrementa la cantidad de almidón nativo presente, la superficie se vuelve más rugosa; en las muestras de DAS10 y DAS10NS50 se observa microporosidad lo cual es adecuado para adhesión y proliferación celular, así como para el intercambio de oxígeno y nutrientes. El hinchamiento en el equilibrio de las películas poliméricas es mayor en los almidones oxidados y se debe a la presencia de mayor cantidad de grupos hidroxilos que se confirma con los análisis de FT-IR. El grosor de las películas depende principalmente del volumen de la mezcla polimérica e influencia la capacidad de absorción de agua de las películas así como también la liberación de la proteína, a medida que es más delgada. El método de superficie de respuesta (RSM) arrojó como resultado una formulación óptima con almidón oxidado con el 5% de peróxido de hidrógeno y 35% de almidón nativo (DAS5NS35); la cual se utilizó para encapsular el extracto de gelatina de Wharton junto con dos formulaciones más en donde se observa la tendencia a liberar mayor cantidad de proteína cuando se utilizan almidones oxidados en las formulaciones. El almidón de camote tanto en su forma nativa como modificada es fácil de obtener; el almidón oxidado es adecuado para la ingeniería de tejidos debido a que las películas poliméricas realizadas con el mismo presentan propiedades adecuadas como capacidad de absorción de agua, y liberación controlada de la proteína encapsulada, así como también, permite realizar películas delgadas y la interacción de grupos carbonilos del almidón oxidado con aminos de las proteínas mejorando las propiedades mecánicas del biomaterial y haciéndolo adecuado para su uso en la ingeniería de tejidos de piel.

Abstract

Starches have been widely used as biopolymers in tissue engineering due to their unique properties such as biocompatibility and biodegradability; nonetheless, sweet potato starch has not been researched in this field. Therefore, films based on oxidized sweet potato starch mixed with PVA and glycerin as plasticizers have been developed to encapsulate a protein extract from Wharton's Jelly. A design of experiments (DOE) was made using BSA as a model protein to analyze scaffolds properties. Films and starches were characterized by Fourier transform infrared (FTIR) which allowed to see interactions between carbonyl groups formed in the oxidation of the starch with amine groups from BSA as well as confirming starch oxidations, scanning electron microscopy (SEM) for film surfaces, optic microscopy for native starch morphology, and analytical methods to determine the optimal formulation of the films according to the response surface methodology (RSM) based on swelling and protein release at equilibrium, and thickness of the scaffolds. For all formulations a rough surface was obtained and formulations with oxidized starch using 10%v/v of H_2O_2, present micropores which may be suitable for cell adhesion and proliferation as well as oxygen and nutrients exchange; while NS is present, roughness in films increased and micropores are not present. The water uptake is much better with oxidized starches than native starch due to its hydroxyl groups showed in the FT-IR spectra. Thickness of the films depends on the volume of the polymeric suspension and influence the swelling capacity; as films are thicker, less water is absorbed. According to the response surface methodology (RSM), the optimal formulation is oxidized starch with 5%v/v of H_2O_2 of and 35% of native starch (DAS5NS35) which was used to encapsulate Wharton's Jelly extract; also, two more compositions were developed for Wharton's Jelly extract encapsulation, the study showed a tendency to release a bigger quantity of proteins when less NS is used. Sweet potato starch in its native and oxidized form is easy to obtain and oxidized starch has potential for tissue engineering as films developed with it can encapsulate a protein extract and release it as well as create bonds between carbonyl groups from oxidized starch and amine groups from proteins which improve mechanical properties of the films. These films fulfill the requirements for swelling and thickness which is adequate for wounds healing and skin tissue engineering.

Keywords: Wharton's Jelly, skin wounds, scaffolds, starch, tissue engineering.

Development of a Film Based on Oxidized *Ipomea Batatas L.* Starch with Protein Encapsulation for Potential Skin Tissue Engineering Applications

Daniela Viteri N., José Álvarez B.

Table of Contents

Resumen

Los almidones han sido utilizados ampliamente como biopolímeros en la ingeniería de tejidos debido a sus propiedades únicas, su biocompatibilidad y biodegradabilidad, sin embargo, el almidón de camote no ha sido investigado en este campo. Por estas razones se plantea realizar películas poliméricas a base de almidón de camote oxidado con PVA y glicerina para encapsular un extracto proteico de la gelatina de Wharton. Se utilizó un diseño experimental utilizando BSA como proteína modelo para analizar las propiedades de los apósitos. Tanto los almidones como las películas poliméricas fueron caracterizadas por espectroscopías infrarrojas por transformadas de Fourier (FTIR), en donde se observan interacciones de los grupos carbonilo de los almidones oxidados con los grupos amino de las proteínas en la posible formación de bases de Schiff, así como se confirman las oxidaciones de los almidones en base a las vibraciones de los grupos aldehídos carbonilos. La microscopía electrónica de barrido (SEM), se utilizó para las superficies de los films y la microscopía óptica para observar la morfología del almidón nativo. Se utilizaron métodos analíticos para determinar la mejor composición de las películas poliméricas basándose en el método de superficie de respuesta en donde las variables de salida fueron el hinchamiento y liberación en el equilibrio y el grosor de las películas, y las variables de entrada fueron el volumen de la mezcla polimérica, el grado de oxidación del almidón y la cantidad de almidón nativo, manteniendo constante el porcentaje de PVA (2%w/v), glicerina (2% v/v) y BSA (5%w/w del total del almidón). En todas las formulaciones se aprecian superficies uniformes rugosas en las imágenes generadas por el SEM, se puede apreciar de igual forma que a medida que incrementa la cantidad de almidón nativo presente, la superficie se vuelve más rugosa; en las muestras de DAS10 y DAS10NS50 se observa microporosidad lo cual es adecuado para adhesión y proliferación celular, así como para el intercambio de oxígeno y nutrientes. El hinchamiento en el equilibrio de las películas poliméricas es mayor en los almidones oxidados y se debe a la presencia de mayor cantidad de

grupos hidroxilos que se confirma con los análisis de FT-IR. El grosor de las películas depende principalmente del volumen de la mezcla polimérica e influencia la capacidad de absorción de agua de las películas así como también la liberación de la proteína, a medida que es más delgada. El método de superficie de respuesta (RSM) arrojó como resultado una formulación óptima con almidón oxidado con el 5% de peróxido de hidrógeno y 35% de almidón nativo (DAS5NS35); la cual se utilizó para encapsular el extracto de gelatina de Wharton junto con dos formulaciones más en donde se observa la tendencia a liberar mayor cantidad de proteína cuando se utilizan almidones oxidados en las formulaciones. El almidón de camote tanto en su forma nativa como modificada es fácil de obtener; el almidón oxidado es adecuado para la ingeniería de tejidos debido a que las películas poliméricas realizadas con el mismo presentan propiedades adecuadas como capacidad de absorción de agua, y liberación controlada de la proteína encapsulada, así como también, permite realizar películas delgadas y la interacción de grupos carbonilos del almidón oxidado con aminos de las proteínas mejorando las propiedades mecánicas del biomaterial y haciéndolo adecuado para su uso en la ingeniería de tejidos de piel.

Abstract

Starches have been widely used as biopolymers in tissue engineering due to their unique properties such as biocompatibility and biodegradability; nonetheless, sweet potato starch has not been researched in this field. Therefore, films based on oxidized sweet potato starch mixed with PVA and glycerin as plasticizers have been developed to encapsulate a protein extract from Wharton's Jelly. A design of experiments (DOE) was made using BSA as a model protein to analyze scaffolds properties. Films and starches were characterized by Fourier transform infrared (FTIR) which allowed to see interactions between carbonyl groups formed in the oxidation of the starch with amine groups from BSA as well as confirming starch oxidations, scanning electron microscopy (SEM) for film surfaces, optic microscopy for native starch morphology, and analytical methods to determine the optimal formulation of the films

according to the response surface methodology (RSM) based on swelling and protein release at equilibrium, and thickness of the scaffolds. For all formulations a rough surface was obtained and formulations with oxidized starch using 10%v/v of H_2O_2, present micropores which may be suitable for cell adhesion and proliferation as well as oxygen and nutrients exchange; while NS is present, roughness in films increased and micropores are not present. The water uptake is much better with oxidized starches than native starch due to its hydroxyl groups showed in the FT-IR spectra. Thickness of the films depends on the volume of the polymeric suspension and influence the swelling capacity; as films are thicker, less water is absorbed. According to the response surface methodology (RSM), the optimal formulation is oxidized starch with 5%v/v of H_2O_2 of and 35% of native starch (DAS5NS35) which was used to encapsulate Wharton's Jelly extract; also, two more compositions were developed for Wharton's Jelly extract encapsulation, the study showed a tendency to release a bigger quantity of proteins when less NS is used. Sweet potato starch in its native and oxidized form is easy to obtain and oxidized starch has potential for tissue engineering as films developed with it can encapsulate a protein extract and release it as well as create bonds between carbonyl groups from oxidized starch and amine groups from proteins which improve mechanical properties of the films. These films fulfill the requirements for swelling and thickness which is adequate for wounds healing and skin tissue engineering.

Keywords: Wharton's Jelly, skin wounds, scaffolds, starch, tissue engineering.

1. Introduction

Chronic skin wounds, genetic skin disorders, burns and diseases as diabetes mellitus may result in skin loss; specially burns and scalds cause wounds with substantial areas of skin damage, usually without the possibility of skin regeneration (1). According to the world health organization (WHO) burns are a global health problem, and non-fatal burns are a leading cause of morbidity, prolonged hospitalization, disfigurement and disability. A burn is an injury to the skin or other organic tissue caused by heat, radiation, radioactivity, electricity, friction or chemicals (2). Another skin damage is the diabetic foot in patients with diabetes mellitus. This is a severe chronic complication that consists of lesions in the deep tissues. As diabetic patients lose regenerative capacity, depending on their diabetes type the complications in the disease can cause the amputation of the lower limbs. The study made by Zhang et al., reports that global diabetic foot prevalence is 6.3% reporting more cases in males than females (3). If the wound is not treated correctly it can cause infections affecting the patient's quality of life.

Traditional ways to heal wounds are creams, gauze, natural extracts that can be herbal compounds or animal derived compounds, living organisms and silver (4). Nowdays traditional medicine has also been used to create optimal conditions for tissue regeneration using natural extracts that have been combined with natural polymers in tissue engineering investigations to promote the healing process (1,5–7). Available biopolymers as polylactic-acid (PLA), polycaprolactone (PCL), polyacrylonitrile (PAN) can result in a high cost, therefore; researchers have been studying the use of those biopolymers, including polysaccharides such as gelatin, starch, chitosan, alginate and pectin to reduce the cost of the potential biomaterials technologies (8–10).

Researchers have discovered interesting properties of some polysaccharides in tissue regeneration; one example is the chitosan cross-linked with *Aloe Vera* to form hydrogels able

to deliver drugs to the body, or to build films that help with tissue regeneration in the case of burns or wounds. Their biocompatibility and the cellular viability are high, so these films can be used in biomedical applications, also there are studies with pectin and alginate with useful properties for tissue engineering (8,11–14).

The development of new biomaterials for tissue engineering, especially for skin, needs to fulfill some requirements as they must be capable of absorbing exudates and keep a moist environment that enhances the growth of new granulation tissue, so as to make the wound healing process efficient. Moreover, it should be biocompatible, non-antigenic, biodegradable, and have the adequate porosity to help the cell proliferation (1,15). Therefore, the use of gelatin-starch hydrogels (13), carboxymethyl cellulose-PEG hydrogels (16), nanofibrous scaffolds with Emu oil (6), polyvinyl alcohol (PVA)-carboxymethyl cellulose and tamarind gum based films (17) and other studies have been developed to reach those properties.

The starches have been used in the pharmaceutical industry, where they have applications in the manufacturing of soft capsules without gelatin, as bone wax, porous scaffolds and as bio-absorbable materials, such as hydrogels to cure wounds (18,19). One of the most common problems with starch is its instability in water that is why they are mixed using cross-linking methods with plasticizers like vinyl monomers (20). Most of the starches that have been studied are from corn, cassava or potato, but very little has been done with *Ipomea batatas L*, a purple tuber from the Convulaceae family commonly produced in Ecuador. To avoid starch instability in water, it can be modified using an oxidation method with hydrogen peroxide, improving its mechanical properties, giving a better stability in water and functionalizing the biomaterials with carbonyl and carboxyl groups (21–23). Despite having promising properties, starches must be combined with bioactive compounds to potentiate tissue regeneration.

There are studies of some plant extracts, such as *Aloe Vera*, drugs and proteins to increase cellular regeneration and accelerate the healing process. The epithelial growth factor is one of the proteins contained in Wharton's Jelly, extracted from the umbilical cord. Lately has been

reported that the use of stem cells from this jelly in regenerative medicine, result in promising treatments in human pathologies, hence the reason for their being one of the most investigated perinatal sources. Studies about Wharton's Jelly show that the stem cells contained there are similar to the ones in the bone marrow, one of the advantages is that the process to get this cells is easier and without damage to the donor; also those cells are easily to differentiate and get more therapeutic applications (24–26). However, working with these cells could cause serious limitations to the commercial success of a skin tissue engineering product. Instead the growth and differentiation factors they secret could be used, in order to produce functional scaffolds (films) that could be mass produced without using the cells themselves.

Therefore, the aim of this study was to develop a film based on oxidized *Ipomea batatas L.* starch, for the encapsulation of a protein extract of Wharton's Jelly from umbilical cord which could potentially be used for skin tissue regeneration.

2. Materials and methods

2.1. Starch Extraction

I*pomea batatas l.,* a purple tuber known as *camote* in Ecuador or sweet potato in other parts of the world, was used to extract the starch. Briefly, tubers were peeled, cut into 2-cm pieces, and homogenized in a blender, using distilled water at 250 grams per 100 mL. The homogenate was filtered, and the starch was allowed to precipitate. The starch was washed three times with distilled water, discarding the supernatant, and following the same precipitation procedure. After the third wash, the rinsing with 70% v/v ethanol was carried out, and dried at 40 °C. Starch yield is calculated following the protocol of Elmi Sharlina, et al. (27) with the following equation:

$$Starch\% = \frac{mass\ of\ extracted\ starch\ (g)}{mass\ of\ fresh\ tubers\ (g)} \times 100 \quad [1]$$

2.2. Starch modification

Starch modification was performed through hydrogen peroxide (H_2O_2) oxidation. Three solutions of hydrogen peroxide at 3, 5 and 10% v/v in distilled water were prepared. At the same time, the starch was washed with ethanol 70% v/v and twice with distilled water to sterilize it; all the materials used were sterilized with ethanol 70% v/v as well.

A 2% w/v solution of starch in distilled water was gelatinized at 80°C for 30 min, under moderate agitation. Then, it was cooled in a water bath until 25°C. The oxidation process was carried out under moderate agitation and dark environment. The initial pH was adjusted to a value of 7, using 0.1M solutions of NaOH and HCl. For every 100 mL of the starch suspension, 6.25 mL of the H_2O_2 solution, at a given concentration, were added drop-wise, in a period of 1h, maintaining the pH at 7.0. When the oxidation process ended, the mixture was centrifuged at 5000 rpm for 5 min. The supernatant was discarded, then it was washed twice more with distilled water. The dialdehyde starch (DAS) was spread in silicon molds and dried in an oven at 40°C for 24-72 hours until constant weight.

2.3. Starch characterization

2.3.1. Optical Microscopy

Starch granules were analyzed in a LEICA DM500 microscope. The granule size was calculated using the microscope software, LAS EZ. For every picture, 100 measurements were collected, and an average was made.

2.3.2. Determination of carbonyl and carboxyl groups

The modified starch was characterized estimating the amount of carbonyl and carboxyl groups to ensure that a modification had been made. For carbonyl groups, an adaptation of the protocol proposed by Smith in 1967 was carried out (28), using 1g of modified starch with 25mL of distilled water. The mixture was heated until gelatinization, and cooled to room temperature, the pH was adjusted to 3.2 with HCl 0.1M. After that, 3.75 mL of hydroxylamine

hydrochloride solution (25g of hydroxylamine hydrochloride + 100 mL of NaOH 0.5M in a 500mL solution) were added, and the mixture was left in the oven at 40°C for 4h. Then, it was titrated potentiometrically with 0.1M HCl until pH of 3.2. The amount of carbonyl groups was calculated using the following equation:

$$\frac{CO}{100GU} = \frac{(V_b - V_s) \times M \times 0.028 \times 100}{W} \quad [2]$$

Where V_b is the titration volume of the blank (native starch, NS), V_s the titration volume of the sample, M the molarity of the HCl and W the weight of the sample dry basis.

In a similar procedure, the carboxyl groups where determined using the protocol proposed by Parovouri, et. al., in 1995 (29), using 1g of oxidized starch in 60mL of distilled water, the mixture was heated until gelatinization, followed by titration, to a value of pH 8.2 with NaOH 0.01M. Carbonyl groups were determined with the following equation:

$$\frac{COOH}{100GU} = \frac{(V_s - V_b) \times M \times 0.045 \times 100}{W} \quad [3]$$

Where V_b is the titration volume of the blank (native starch, NS), V_s the titration volume of the sample, M the molarity of the HCl and W the weight of the sample dry basis.

2.3.3 Fourier Transformed Infrared Spectroscopy (FT-IR) analysis

The samples of native starch (NS), oxidized starch at 5% H_2O_2 (DAS5), oxidized starch at 10% H_2O_2 (DAS10) and different film formulations (section 2.4) were analyzed with a Cary 630 FTIR Spectrometer from Agilent Technologies.

2.4 Design of Experiments (DOE) and Preparation of Films

A statistically designed set of experiments was carried out using the response surface methodology (RSM) to minimize the number of experiments and maximize the amount of data generated. Through this analysis, the effect of each parameter in the film formulation could be evaluated (30). It is important to select an appropriate design, not only based on the factor or

independent variables but also on the availability of resources for each experiment (31). The RSM is a collection of statistical tools and techniques for constructing an approximate functional relationship between response variables and a set of design factors (32).

Using the software JMP, the model was prepared with 34 experiments using a composite design method with a 5 center point model described in **Table 1**. Center points are used to determine the experimental error and the reproducibility of the data, which is assumed to be the same for the other experiments as well (33). The input parameters were volume of the polymeric suspension, oxidation degree and amount of native starch; the outputs were film thickness, protein release at equilibrium and swelling at equilibrium.

For the DOE, bovine serum albumin (BSA) obtained from Sigma-Aldrich was used as a model protein for encapsulation. A stock solution was made for BSA with 25 mg per mL in distilled water and 10% w/v Poly(vinylalcohol) (PVA) obtained from Sigma-Aldrich as Mowiol® 18-88, $M_W \sim 130,00$, in distilled water. Each film was made according to **Table 1** (DOE). Constant parameters were PVA (2%wt/v), glycerin (2%v/v) and BSA (5 %wt of the total starch amount).

 First, the amounts of native and oxidized starch were weighed and gelatinized with distilled water under moderate agitation at 80°C for 15min and cooled to room temperature. The slurry was transferred to a 50 mL conical tube and allowed to cool to room temperature; then PVA, glycerin and BSA solutions were added to the polymeric mixture, followed by vortex homogenization for 30 seconds. The resulting mixture was placed in polystyrene petri dishes, stored in a freezer at -14°C for 24h, and subsequently dried at 40°C overnight according to drying method #4 shown in **Table 4**. Once dried, films were stored in the refrigerator at 4°C.

Table 1. Design of experiments to study the effect of the oxidation degree, amount of native starch and volume of polymeric suspension in the composition of each film considering the constant variables to be 2% wt/v PVA, 2% v/v glycerin and 5% wt/wt BSA of the total amount of starch. Design based on the face centered composite design.

Face centered Central Composite Design

Factor	Levels				
	a	-	0	+	A
	-α	-1	0	1	α
Oxidation degree [%H2O2] *	0	0	5	10	10
NS [wt%] **	0	0	50	100	100
Volume [mL]	12	12	18.5	25	25

* Oxidation degree is expressed as the concentration of H_2O_2 (%v/v) used in the process of modification

** NS: percentage of native starch

2.5 Film characterization

2.5.1 Film Thickness

The thickness (μm) of the film was determined using a micrometer (Mitutoyo, Tokyo, Japan). The film was dried at 37°C overnight before it was measured, and the thickness was determined as the average of measurements in 8 random locations.

2.5.2 Swelling and protein release of the film

Films were dried in an oven at 37°C overnight to eliminate moisture. They were then weighed, and 4 squares of 0.7x0.7cm were cut from each film. These squares were placed in 24 well-plates, and 1 mL of Phosphate Buffer Saline (PBS 0.01M, pH 7.2) was added to each well. During the first hour of the experiment the film was weighted every 15 minutes, and a known volume of the supernatant was collected and replaced with fresh PBS. After that, samples were weighed at 5, 24, 48, and 72 hours, and supernatant was collected. The stability was assumed to be at 72 hours, as demonstrated in previous tests (data not shown).

The swelling ratio was calculated as follows according to Li, et al (18):

$$SW = \frac{M_t - M_0}{M_0} \times 100\% \quad [4]$$

Where SW is the swelling percentage, M_t is the weight of the sample at equilibrium and M_0 is the initial weight of the sample.

The protein release was determined via the Bradford method. A calibration curve was made according the parameters provided for Sigma-Aldrich Bradford reagent for a 96-wells assay (34). Each sample was prepared in the 96 well-plates, and they were incubated for 25 minutes. Absorbance at 560 nm was measured using an ELISA plate reader (Sirio S Reader). Absorbance data was converted to concentration using a calibration curve made with solutions of known BSA concentrations, and the cumulative release was calculated.

2.6 Scanning Electron Microscopy (SEM)

All samples were analyzed with JEOL JSM-IT300 scanning electron microscope, using the program MP-96040EXCS External Control Software. Starch samples at 50 Pa and 5 kV and films samples at 30 Pa and 5 kV to avoid sample damage by the electron beam.

2.7 Encapsulation of Wharton's Jelly Extract

A protein extract from Wharton's jelly was prepared by cutting human umbilical cord into pieces, washed with PBS, and homogenized in a blender. The resulting product was filtered and stored at 4°C. Protein concentration was measured using Bradford, as previously explained.

Optimal compositions for the films according to the DOE were used, along with control formulations that consisted of: WJ1, DAS oxidized at 5%, PVA and glycerin; WJ2, DAS oxidized at 5% and 35 wt% NS, PVA and glycerin, and WJ3, NS, PVA and glycerin.

These films were prepared following the same protocol as described in section 2.4., with the difference of using 24-well plates instead of petri dishes because of the limited availability of

the WJ extract. An area relation was used to determine the volume of slurry for each formulation; $435 \frac{\mu g}{mL}$ of WJ extract were encapsulated. Films were dried with method #4 (**Table 4**).

3. Results and discussion

3.1 Starch extraction

The process of starch extraction from *ipomea batatas L.* presented a yield of 14.44%, with respect to the total mass of the tuber processed. Figure 1 shows the morphology of the granules. *Ipomea batatas L.* starch had an average size of $(23.18 \pm 7.25) \mu m$, with variations from $8.69 \mu m \ to \ 46.79 \mu m$, similar values to those reported by Oluwatooyin et al., from $2 - 60 \mu m$ in samples of *ipomea batatas L* (35). The granules of *ipomea batatas L.* starch are smaller than those of potato or cassava with sizes around $5 - 100 \mu m$ and $3 - 43 \mu m$, respectively (36).

 The starch granules presented a spherical bell form as seen in **Figure 1** which is different from other starches as potatoes or cassava that present ovoidal forms. This corroborates the findings from previous studies that have described this unusual shape (35,37).

The most important components in the starch are amylose and amylopectin, which are present in compositions of 19.6% amylose and 80.4% amylopectin in Mexican sweet potato (36). For oxidations with hydrogen peroxide the amount of amylose and amylopectin is important according to Zhang, et al., who estates that amylopectin molecules are more prone to oxidation than amylose molecules (22).
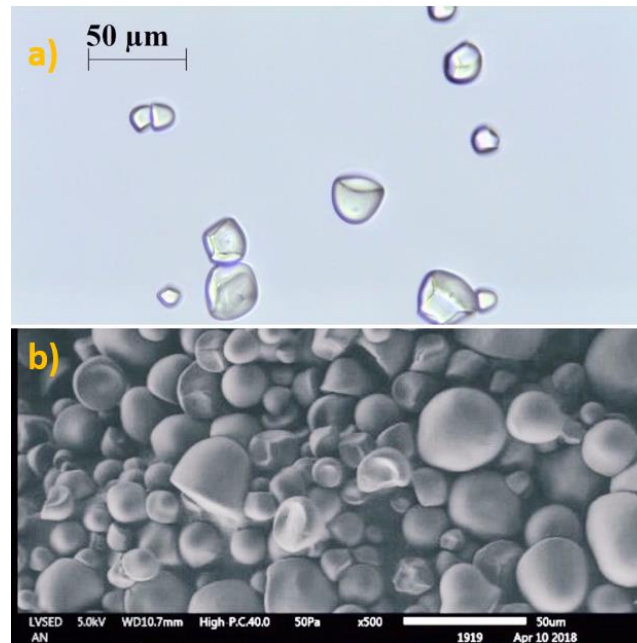
Figure 1. *Ipomea batatas L.* starch granules observed under: a) Optic microscopy at 40X, and b) SEM at 500X.

3.2 Starch modification

3.2.1 Carbonyl and carboxyl groups present in the starches

Starch chemical modification is widely used in food and non-food industry as it gives functional groups to the starch, changing its properties and thereby, its functionality (22). The functional groups obtained by oxidation are carbonyl and carboxyl, and their values for the oxidation of sweet potato starch in this work are shown in **Table 2**. The amount of carbonyl and carboxyl groups depends on the pH value, temperature, and time of reaction, among others. It is a complex reaction, as described by Salmi, et al. in their study for a mathematical modeling (38). In the present study, it can be observed that oxidation with H_2O_2 at 5 and 10% v/v yields carbonyl and carboxyl groups comparable to the study made by Zhang, et al., where the highest carbonyl and aldehyde groups where obtained in the oxidation with molar ratio of H_2O_2/starch < 0.7 which is equivalent to a 10.53% H_2O_2 percentage (23).

Other studies also show the great capacity of H_2O_2 to oxidize the hydroxyl groups present in the backbone of the starch to carbonyl and carboxyl groups, some methods have been optimized using catalysts to obtain a great amount of carbonyl groups (22,39,40). As seen in

Table 2, the amount of carboxyl groups is smaller than carbonyl groups, which is good as the purpose of the oxidation is to obtain carbonyl groups as they can form Schiff bases with the amine groups from proteins.

Table 2. Carbonyl and carboxyl group content in the dialdehyde sweet potato starch.

H_2O_2 Percentage [%v/v]	Carbonyl [CO/100GU]	Carboxyl [COOH/100GU]	Total oxidation [CO+COOH/100GU]
3	0.157 ± 0.040	0.023 ± 0.001	0.220 ± 0.327
5	0.432 ± 0.010	0.066 ± 0.003	0.508 ± 0.013
10	0.534 ± 0.022	0.070 ± 0.002	0.627 ± 0.021

3.2.2 FT-IR analysis of the native and modified starch

Samples of each oxidized starch (DAS) and native starch (NS) were evaluated using FT-IR. For the native starch extracted, a comparison was made with the standard starch of sweet potato provided by the software's library, shown in **Figure 2**. The spectrum of extracted starch differs significantly from that of the standard, which can be due to impurities that remain during the extraction process such as proteins, lipids, fibers, non-starch polysaccharides, and pectins, which are particularly important in sweet potato (41). As seen in **Figure 3**, in the spectra for oxidized starches the impurities seem to have diminished; this happens because of the fact that hydrogen peroxide is a bleaching agent that promotes the degradation of many impurities, and even delignification in biomass, hence its industrial applications for product purification (42).

DAS spectra, shown in **Figure 3** present bands at 1000 – 1200 cm^{-1} attributed to C-O bond stretching of the starch, and, at 1640 cm^{-1} , a band related to a tightly bond of water in starch (43). The peak at 1735 cm^{-1} is attributed to C=O stretching vibration, this is due to the increasing aldehyde contents in DAS and confirms the oxidation (21,22). This peak can be seen in **Figure 3** for DAS5 which describe the presence of carbonyls and carboxyl groups. Peaks at 2930 cm^{-1} are due to C-H asymmetrical stretching and 1210 cm^{-1} C-O bending vibrations. Peaks at 2800 cm^{-1} also represents C-H aldehydes bonds, in **Figure 3**, DAS10 reveals slightly

more aldehydes in this section than DAS5. According to the results in **Table 2**, DAS10 has slightly more carbonyl groups than DAS5, but the spectra of this oxidized starch does not present the peak at 1735 cm^{-1} which is characteristic for carbonyl and carboxyl groups.
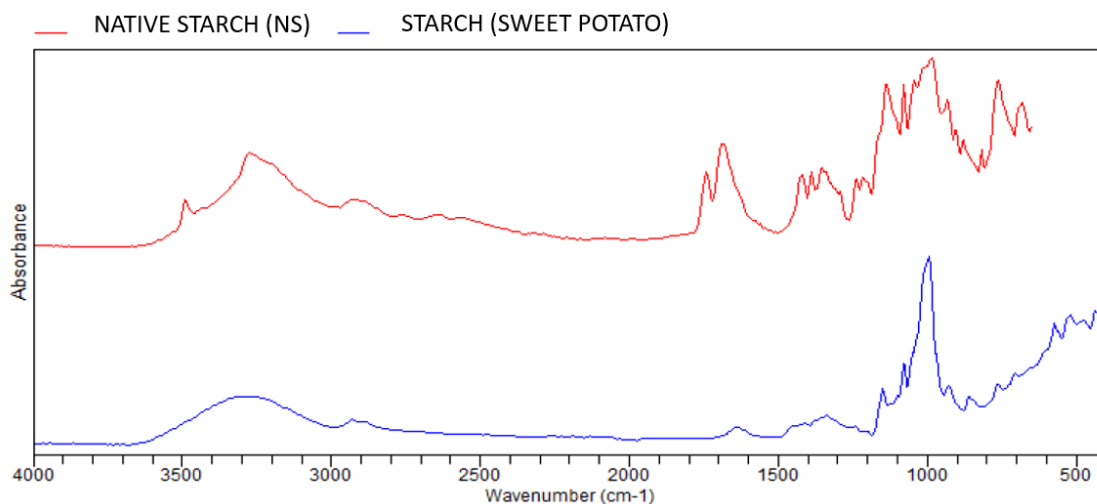
Figure 2. Comparison between extracted native starch with standard sweet potato starch FT-IR spectra.
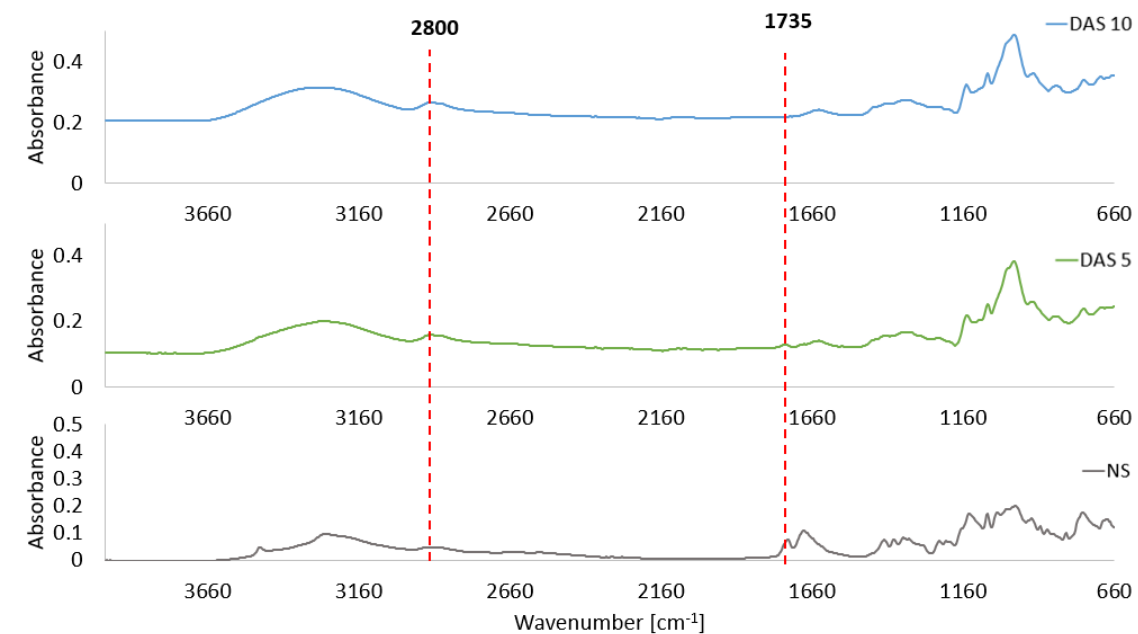
Figure 3. FT-IR spectra of oxidized starch with 5% (DAS5) and 10% of H$_2$O$_2$ (DAS10) compared with native starch (NS).

3.3 Development of the production method of the films

The production method was evaluated according to the film's physical characteristics by varying the drying time and temperature. Assays were carried out according to **Table 3**, and the drying method was chosen according to **Table 4**. As the films were to encapsulate proteins, the time of drying and temperature were considered as important parameters to avoid protein denaturalization, so the drying method chosen for the films was freezing the polymeric suspension at -14°C for 24 h and then drying at 40°C (# 4) and the compositions with 5%wt of starch (NS and DAS), 2% wt/v of PVA and 2% v/v of glycerin (D and F). In **Figure 4** films resulting from different drying methods are observed, the ones presenting cracks correspond to drying methods 1 (A) and 3 (C) where films are dried under room temperature and oven respectively without freezing; therefore, the final methodology was picked to be the method 4 that freezing the films before drying them in the oven, those yielded continuous and transparent films and the time of drying does not exceed 24 h.
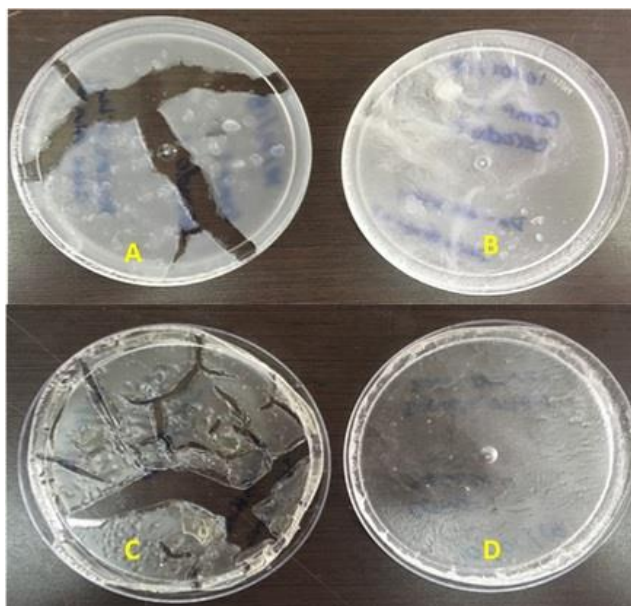
Figure 4. Films obtained by the drying methods presented in **Table 4**: A) method #1, room temperature drying, B) method #2, freezing and room temperature drying, C) method #3, oven at 40°C and D) method #4, freezing and dried at 40°C.

Table 3. Formulations to define the composition of each film according to macroscopic physical characteristics.

Composition	PVA [wt/v%]	Glycerin [v/v%]	NS* [wt/v%]	DAS** [wt/v%]	Observations on Physical Characteristics
A	2	0	5	0	Rigid and brittle film
B	2	0	10	0	Hard, brittle and rigid film
C	5	0	10	0	Hard, brittle and rigid film
D	2	2	5	0	Malleable and elastic film
E	2	2	10	0	Hard, brittle and rigid film
F	2	2	0	5	Malleable and elastic film
G	2	2	0	10	Hard, brittle and rigid film

* NS: native starch

** DAS: dialdehyde starch

Table 4. Experimental conditions to determine the drying method depending on the time.

Method	Drying procedure	Time [hr]	Observations
1	Room temperature	48 - 72	Slow drying, opaque films with cracks
2	Freezing 24 h at -14°C and then drying at room temperature	24 - 48	Opaque and continuous films
3	Oven at 40°C	12 - 24	Clear films with cracks
4	Freezing 24 h at -14°C and then drying at 40°C	12 - 18	Faster drying method, clear and continuous films

3.4 Design of Experiments (DOE)

Experimental factors were analyzed according to the important responses for the development of films for skin tissue engineering. In this work, the response variables were protein release and swelling at the equilibrium, and thickness of the films. These responses are important as it is not expected that all the protein is released completely, it is expected that amine groups of the protein forms Schiff's bases with carbonyl groups of DASs, so it serves as an extracellular matrix for the cells. Swelling is an important response as the wound needs humidity to heal and the wound would exudate fluids as it heals, so the film needs to absorb a great amount of those exudates (44). Additionally, swelling capacity is directly related to protein delivery (45).
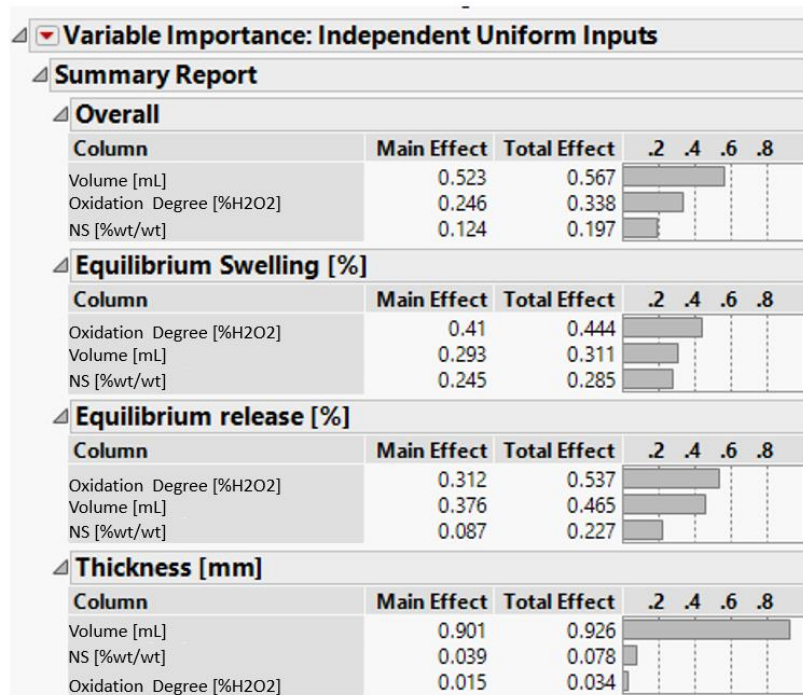
Figure 5. Variable importance of each input variable depending on the output obtained in the experimentation process.

Results from the DOE are shown in **Table 5** where great deviations in central points can be seen, for protein release response which gives a great experimental error as data from the central point variates greatly from one another, for thickness and swelling deviations are low in central points which gives small experimental errors. This DOE was made to see which factor has more importance in the protein release and swelling properties of the film, as well as on the film's thickness. According to **Figure 5**, in the overall analysis, the volume of the polymeric suspension had a greater effect, followed by the degree of oxidation, and lastly, the amount of native starch in the formulation. The parameters with greater effects on each response are also described; for swelling and protein release in equilibrium the degree of oxidation plays the most important role; in the release the effect of the degree of oxidation and volume of polymeric suspension are close, so both are important in the response. Finally, and as expected, the thickness of the film depends on the volume of the polymeric suspension almost in its entirety.
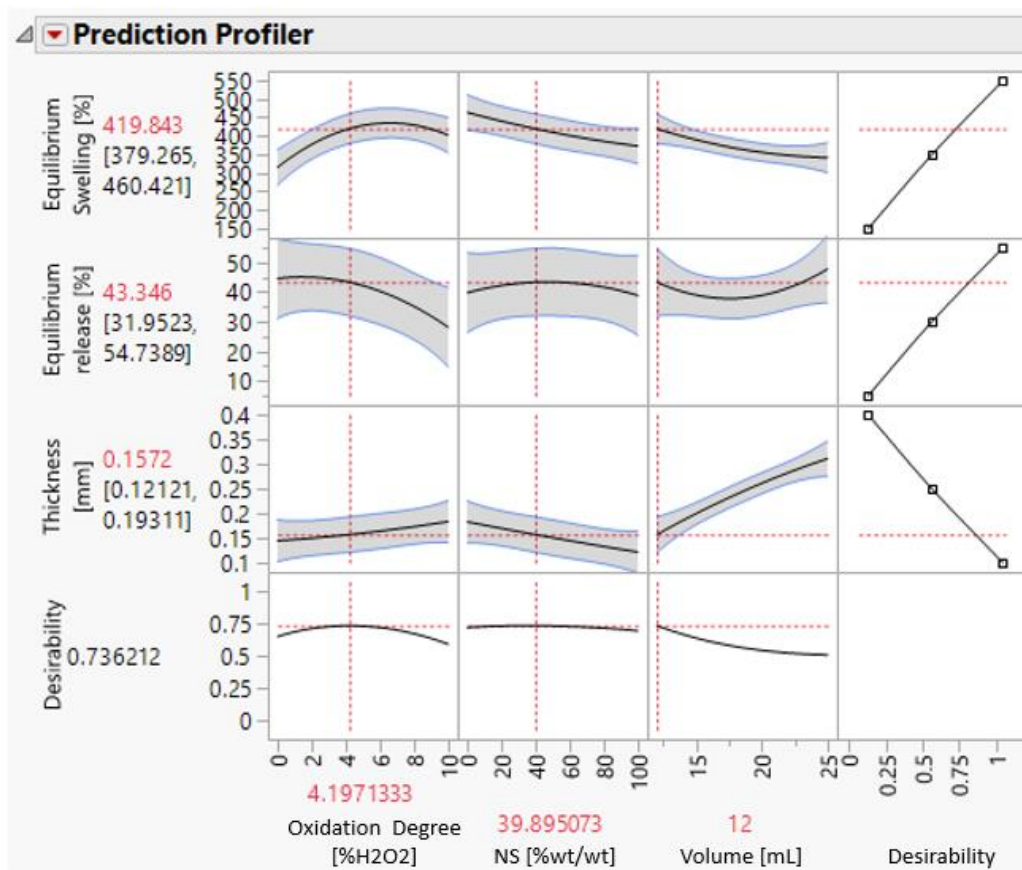
Figure 6. DOE prediction profiles according to experimental data.

In **Figure 6** the influence of each parameter in the responses is described. For swelling in the equilibrium, the degree of oxidation shows a maximum around 7%, and decreases after that. The NS quantity also influences the release, so it presents a maximum when no NS is added to the formulation. For protein release at equilibrium, as the degree of oxidation and volume of polymeric suspension are important parameters, this figure shows the model with each predicted response. As the degree of oxidation increases, the release decreases, despite presenting a maximum around 4%. That is why the prediction of the model shows in red lines that to maximize the swelling and protein release in the equilibrium while minimizing the thickness of the film, the program has predicted that the amount of NS should be approximately 35%, oxidation degree approximately 4% and volume 12mL. The available DAS, however, are oxidized at 5 and 10% so it was decided to use 5% degree of oxidation since it was closest to the optimal value.
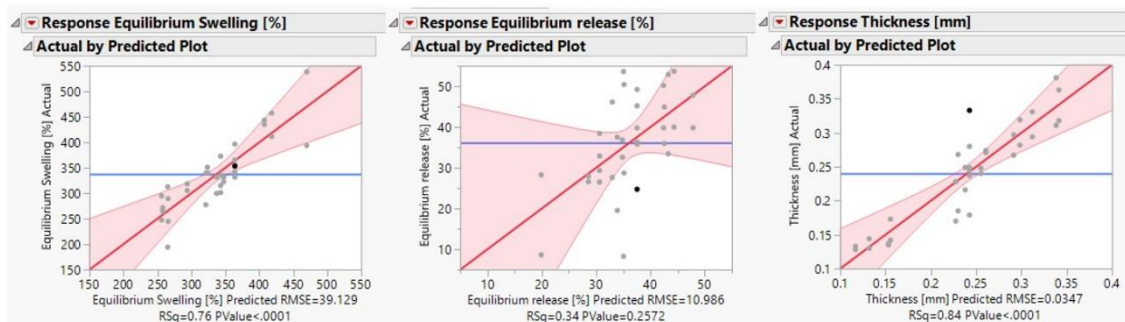
Figure 7. Variability of the responses according to the variables. Actual (grey dots) and predicted data for the model

The predicted model and experimental data are showed in **Figure 7**. It can be seen that the experimental data fits the swelling predicted model as it has a P<0.0001, and the confidence level was established at 95% (P<0.05). For the thickness model, experimental data also fits with a P<0.0001, and the model does not fit the experimental data for the protein release as its P=0.22(30).

As seen in **Figure 3**, the amount of carbonyl and carboxyl in both oxidized starches is not too high, so some hydroxyl groups are still present and those are responsible for water absorption, when the starches contains a high degree of oxidation, most of these groups are used so it decreases the swelling (22). These results are comparable to Nourmohammadi, et al. study, where they developed bioactive composite scaffolds with polycaprolactone, chitosan and oxidized starch; as more DAS were included in the formulations, swelling rates increases due to the presence of more hydroxyl groups from the starch (46). To our knowledge, there are no previous studies that assess protein release with dialdehyde starch.

Table 5. Design of experiments (DOE) responses.

#	Pattern	Oxidation percentage [%H2O2]	NS [wt%]	Volume [mL]	Equilibrium Swelling [%]	Equilibrium release [%]	Thickness [mm]
1	A00	10	50	18.5	340.273	27.921	0.248
2	+−−	10	0	12	393.768	8.627	0.185
3	−+−	0	100	12	305.295	8.284	0.144
4	−++	0	100	25	244.749	26.501	0.381
5	a00	0	50	18.5	312.712	32.580	0.216
6	0A0	5	100	18.5	299.724	27.628	0.228
7	0a0	5	0	18.5	434.898	19.532	0.271
8	0	5	50	18.5	353.367	24.742	0.333
9	A00	10	50	18.5	350.984	26.574	0.240
10	+−−	10	0	12	538.466	28.255	0.268
11	−+−	0	100	12	318.500	53.626	0.130
12	a00	0	50	18.5	194.225	36.856	0.249
13	+++	10	100	25	247.701	44.916	0.319
14	−−−	0	0	12	315.145	53.667	0.142
15	+−+	10	0	25	322.506	50.430	0.318
16	0	5	50	18.5	342.040	39.784	0.249
17	0a0	5	0	18.5	443.371	37.526	0.274
18	−−+	0	0	25	264.475	52.891	0.297
19	0	5	50	18.5	331.694	49.208	0.280
20	00a	5	50	12	411.424	50.197	0.135
21	−−−	0	0	12	335.868	39.981	0.173
22	−++	0	100	25	289.605	38.410	0.311
23	00A	5	50	25	301.515	47.802	0.331
24	+−+	10	0	25	331.648	28.727	0.363
25	++−	10	100	12	277.585	29.328	0.133
26	0	5	50	18.5	396.497	35.787	0.245
27	0	5	50	18.5	365.219	36.323	0.237
28	00a	5	50	12	457.351	39.801	0.137
29	0A0	5	100	18.5	331.470	46.123	0.170
30	00A	5	50	25	372.703	39.802	0.294
31	0	5	50	18.5	355.235	45.212	0.179
32	++−	10	100	12	339.618	32.888	0.128
33	+++	10	100	25	294.881	35.960	0.282
34	−−+	0	0	25	271.598	33.447	0.267

* Center points are highlighted

3.5 Scanning Electron Microscopy (SEM) of the films

Film surfaces were evaluated through SEM for morphological analyses. A sample for five different formulations in **Table 5** were analyzed. Surfaces of the films are uniform, they present rugosity which can be seen in figures 9 – 13.

Samples with DAS10 present micropores which can be seen in **Figure 8**, and micropores are also present for samples with DAS10 and 50% NS in **Figure 9** which can influence the water absorption and helps in the oxygen exchange as those pores are present, corroborating the results from swelling at equilibrium (47). Formulations with DAS10, DAS10 50% NS and DAS5 in **Figure 8**, **Figure 9** and **Figure 10**, respectively, present smoother surfaces, according to previous studies for films with oxidized starch and gelatin from Moreno, et al., the smoothness of the films represent the crosslinking ability of oxidized starch and a great integration between all the components of the films (48). Formulations with DAS5 50%NS and 100% NS in **Figure 11** and **Figure 12**, respectively, present more rugosity than the films described previously. This could be due to insufficient homogenization between all components and caused by the high viscosity of gelatinized NS. For tissue engineering, pores are important as they allow permeability of oxygen and essential nutrients (45), also they allow more water uptake which is beneficial for early stage of wound healing as nutrients and cells will entirely depend on tissue fluids surrounding the wound (49,50). Another important fact with this type of scaffolds is that the roughness is necessary for cell adhesion. Some studies revealed that for osteoblasts rough surfaces shows great cell adhesion and proliferation (51,52); for fibroblasts studies demonstrate that this type of cells prefer rough surfaces instead of smooth ones, as the studies showed more cells in rough surfaces than in smoother ones (45).
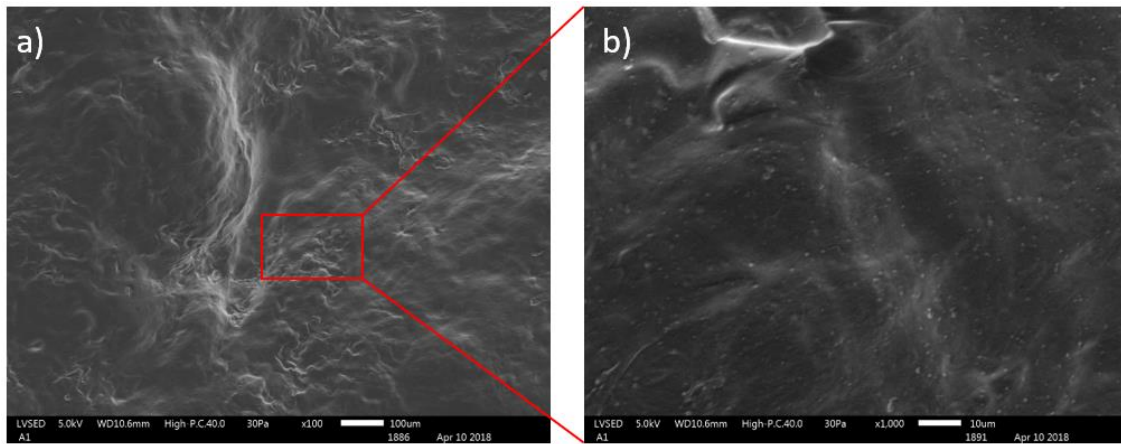
Figure 8. SEM for sample #2, DAS10 + 2% wt/v PVA + 2%v/v Glycerin + BSA. a) 100X, b) 1000X.
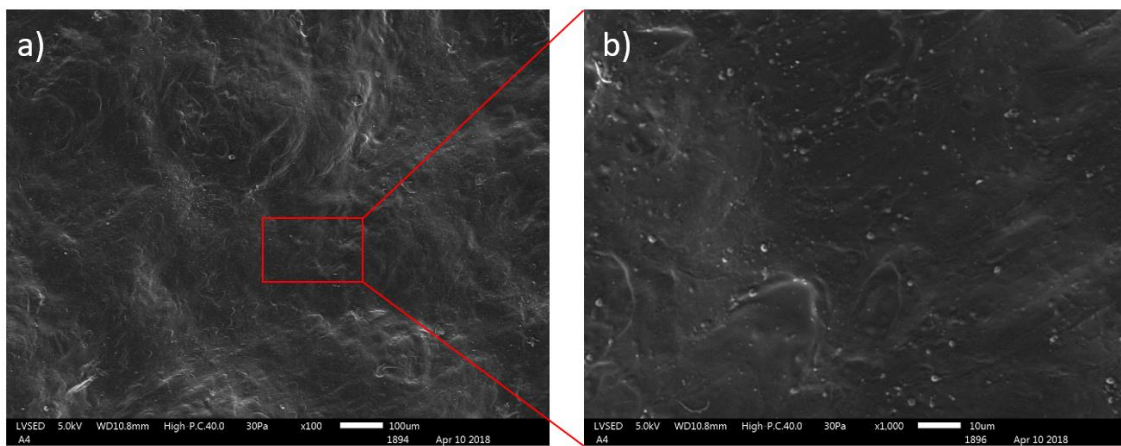
Figure 9. SEM sample #1, DAS10 with 50% NS + 2% wt/v PVA + 2%v/v Glycerin + BSA. a) 100X,
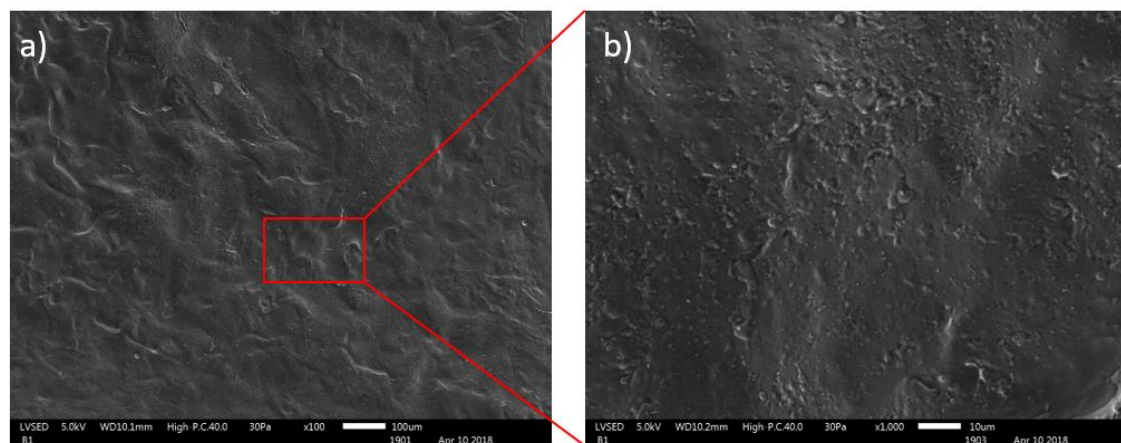
b) 1000X.

Figure 10. SEM for sample # 7, DAS5 + 2% wt/v PVA + 2%v/v Glycerin + BSA. a) 100X, b) 1000X.
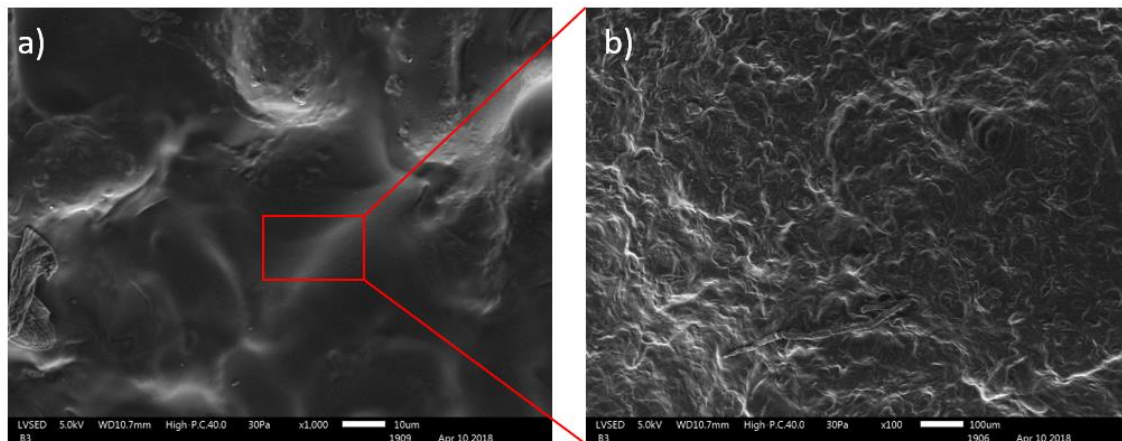
Figure 11. SEM sample #16, DAS5 with 50% NS + 2% wt/v PVA + 2%v/v Glycerin + BSA. a) 100X,
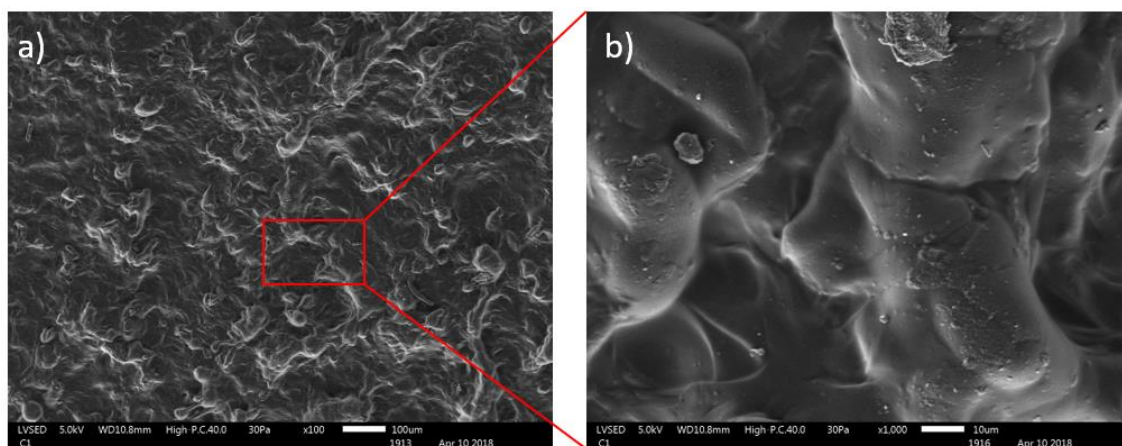
b) 1000X.

Figure 12. SEM for sample #3, 100% NS + 2% wt/v PVA + 2%v/v Glycerin + BSA. a) 100X,

b) 1000X.

3.6 Fourier Transform Infrared Spectroscopy (FT-IR) of the films

This analytical method was used to determine the presence of some important groups and bonds in the films to see how the different formulations influence in its chemical properties. **Figure 13** shows the spectra for the film containing PVA and glycerin with encapsulated BSA, compared to a film containing NS, PVA, glycerin and BSA. Around 1539 cm^{-1} ; it can be observed that there is a difference in the wavenumber which corresponds to N-H bending and C-H stretching vibration of amine II present in the planar peptidic bond vibrational modes of

BSA molecules (45,53). In **Figure 14** and **Figure 15**, at 1539 cm^{-1}, the same pattern is observed as the peak intensity decreases when using more NS. At 1643 cm^{-1} a peak corresponding to C-N bonds that are assumed to correspond to Schiff bases (combination of C-N stretching and C=O bending vibrations) is seen (54). This wavenumber shows a bigger peak when no NS is used, thereby corroborating that it corresponds to Schiff bases formed between the protein and DAS. In **Figure 14** and **Figure 15**, when NS is used at 50%, the interactions C-N decrease, this could be as less carbonyl groups are present Schiff base cannot form with amines from the BSA. Nevertheless, when using the optimal composition with NS 35% these interactions are similar as using no starch (PVAG). This could be due to the availability of carbonyl groups.
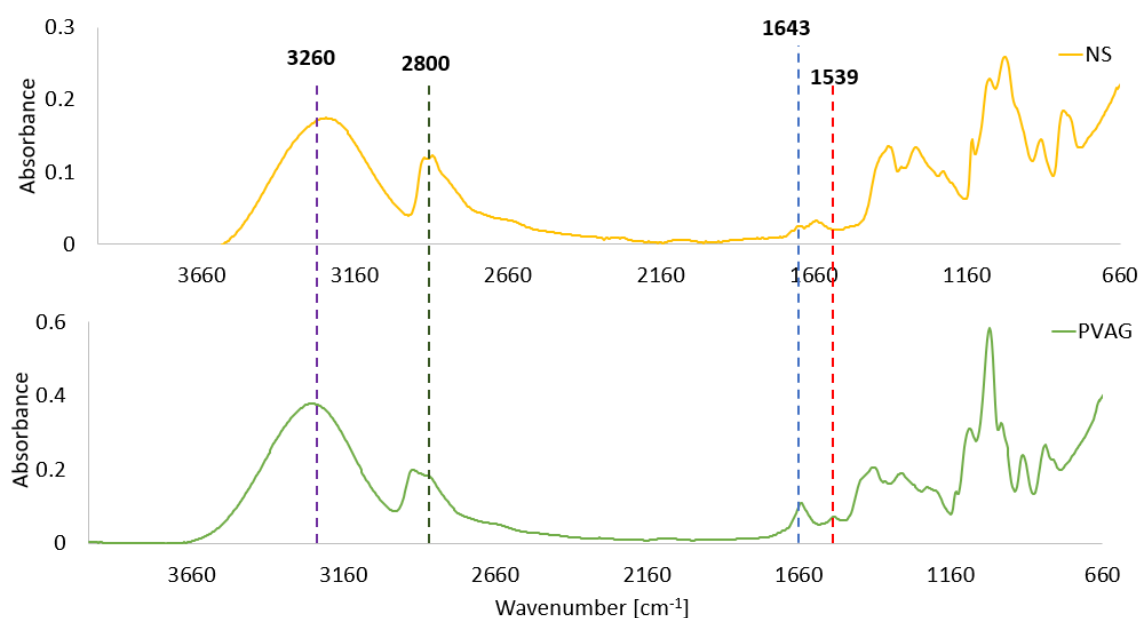
Figure 13. FT-IR spectra of films formulations with only NS, compared with a film containing PVA and glycerin (PVAG).

Peaks around 2800 cm^{-1} correspond to C-H stretching that could be due to aldehyde bonds. According to the spectra for NS in **Figure 13** less C-H interactions are present, similar patterns are shown in **Figure 15** for the presence DAS10NS50; when just DAS10 is present in the film, the intensity of the peaks are close to the ones of PVAG. DAS10 shows a larger peak than the one with PVAG; it may be because of the aldehyde groups in the DAS10. For **Figure 14**, as NS is

present in the formulations, less C-H vibrations around 2800 cm^{-1} can be seen; also, the intensity of the DAS5NS35 is bigger than DAS5. Peaks around 2930 cm^{-1} corresponds to -CH$_2$ vibrations of the glucose unit.
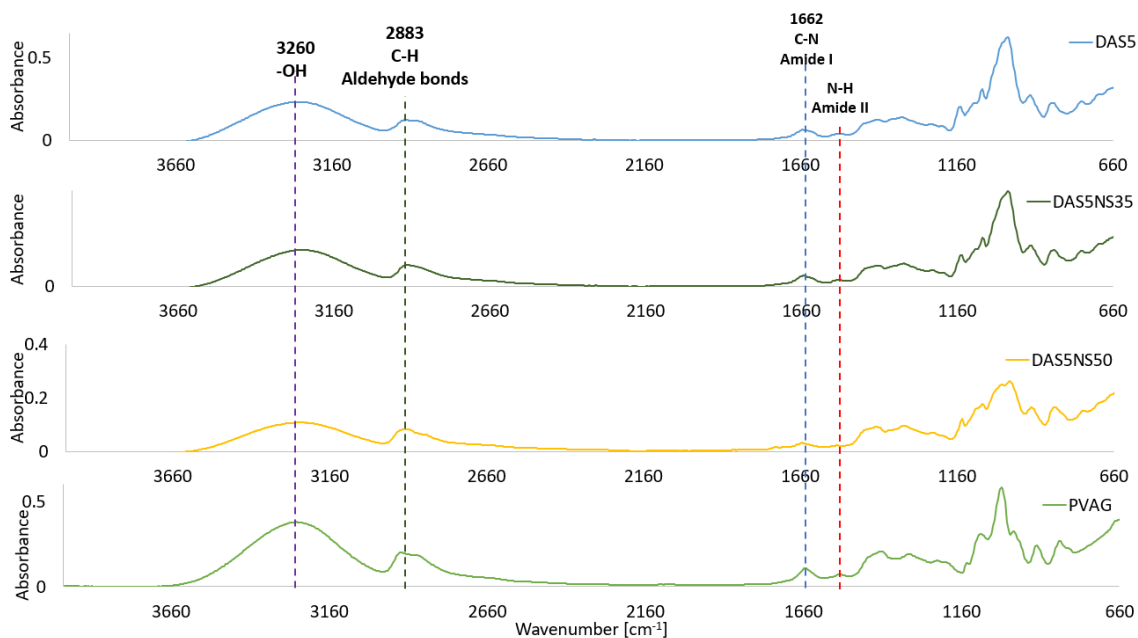
Figure 14. FT-IR spectra of films formulations with only DAS5, DAS5 with 50% NS (DAS5NS50) and the optimal composition with DAS5 and 35% NS(DAS5NS35), compared with a film containing PVA and glycerin (PVAG).

Peaks around 3260 cm^{-1} correspond to hydroxyl groups (-OH), those are from PVA, glycerin and the starches. Hydroxyl groups are responsible for the water absorption in the films (22). Here, there could be a confirmation for the model as less quantity of NS is present more hydroxyl groups are present in the films, so they can uptake more water and the swelling rates increases. Finally, peaks around 1000 cm^{-1} are characteristic for NS, glycerin and PVA, in the three figures below the same pattern is present, when NS is present the peaks are smaller, this could be that the NS is not interacting with PVA or glycerin.
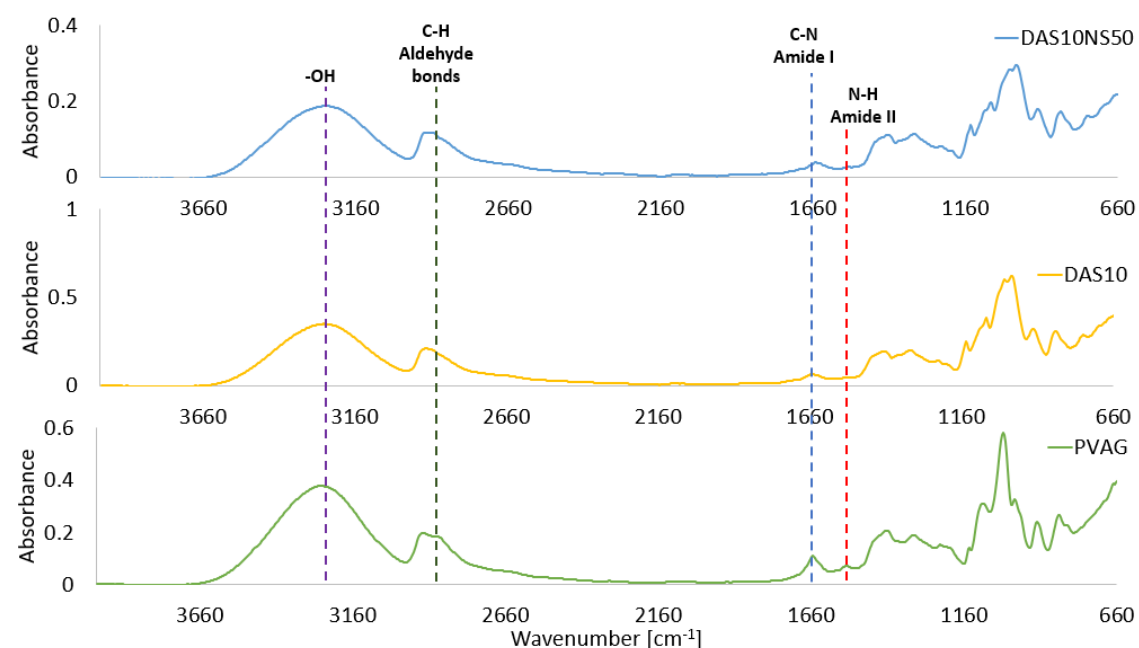
Figure 15. FT-IR spectra of films formulations with only DAS10 and DAS10 with 50% NS

(DAS10NS50), compared with a film containing PVA and glycerin (PVAG).

3.7 Films with Wharton's Jelly extract

According to the analysis of the results from the DOE, the optimal film formulation consisted of DAS oxidized with 5% H_2O_2, native starch content of 35% wt/v, using a volume of 12 mL for the formulation; this would maximize swelling and minimize the thickness of the film. Consequently, this formulation was used to encapsulate the Wharton's Jelly protein extract, along with other compositions of only native starch (NS) and only DAS5 with WJ extract as controls.

According to **Figure 16**, no significant differences between cumulative release profiles are observed; nevertheless, when using greater amounts of NS in the formulation, a tendency to release less amount of proteins is seen. We can't conclude much about WJ1 and WJ2, both seem to be similar due to large standard deviations. For all formulations, proteins were released in a major quantity during the first 4 hours; stability is reached at 48 hours. This result is related to the DOE as NS is present, swelling and protein release rates decreased.
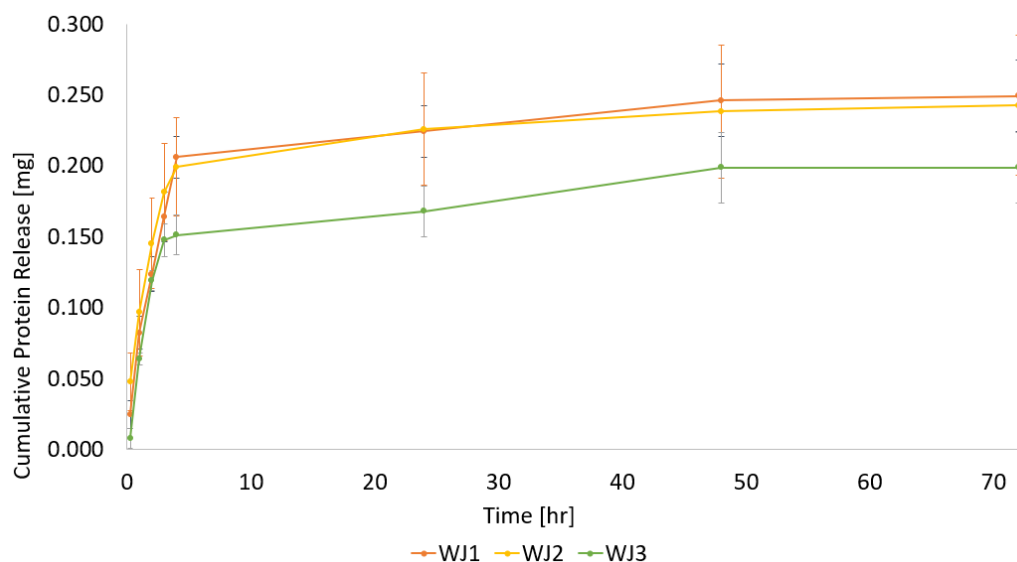
Figure 16. Cumulative protein release essays with different compositions of films and Wharton's Jelly extract. WJ1, contains DAS oxidized at 5%, PVA and glycerin; WJ2, contains DAS oxidized at 5% and 35 wt% NS, PVA and glycerin and WJ3, contains NS, PVA and glycerin.

4. Conclusions and recommendations

The response surface methodology (RSM) for this work gives a model that fits for thickness and swelling parameters; however, for protein release, a new model should be performed, as the predicted model does not statistically fit. According to the DOE the parameter with more effect on the overall system is the volume followed by the degree of oxidation and percentage of NS. Swelling and protein release are responses that have a greater effect with degree of oxidation and are correlated as swelling rates increases the release increases, this is also a good fact as these scaffolds needs to absorb exudates from the wound and promote its healing. FT-IR spectra for the films show that some Schiff bases may be formed when less NS is used, also the peaks for hydroxyl groups may confirm the swelling rates for the films, when they have less NS they absorb more water which is beneficial for wound healing. WJ protein extract was encapsulated correctly and according to the experiments, they may have no relevant difference in the release with the films formulations, this must be evaluated as the standard deviations are too high. Nevertheless, the films compositions performed showed

properties that may be useful for skin tissue engineering and the encapsulated protein extract may be able to release its growth factors and improve healing times. This biomaterial can work for tissue engineering for wound healing purposes, for that, studies for cytocompatibility, cytotoxicity, cell adhesion, biocompatibility, biodegradability and in vitro studies must be performed.

5. Acknowledgments

6. References

1. López Angulo DE, do Amaral Sobral PJ. Characterization of gelatin/chitosan scaffold blended with aloe vera and snail mucus for biomedical purpose. International Journal of Biological Macromolecules [Internet]. 2016;92:645–53. Available from: http://dx.doi.org/10.1016/j.ijbiomac.2016.07.029

2. WHO | Burns [Internet]. Who. World Health Organization; 2018 [cited 2018 Apr 1]. Available from: http://www.who.int/mediacentre/factsheets/fs365/en/

3. Zhang P, Lu J, Jing Y, Tang S, Zhu D, Bi Y. Global epidemiology of diabetic foot ulceration: a systematic review and meta-analysis†. Annals of Medicine [Internet]. 2017;49(2):106–16. Available from: http://dx.doi.org/10.1080/07853890.2016.1231932

4. Pereira RF, Bártolo PJ. Traditional Therapies for Skin Wound Healing. Advances in Wound Care [Internet]. 2016;5(5):208–29. Available from: http://online.liebertpub.com/doi/10.1089/wound.2013.0506

5. Hadisi Z, Nourmohammadi J, Nassiri SM. The antibacterial and anti-inflammatory investigation of Lawsonia Inermis-gelatin-starch nano-fibrous dressing in burn wound. International Journal of Biological Macromolecules [Internet]. 2018;107(2018):2008–19. Available from: http://dx.doi.org/10.1016/j.ijbiomac.2017.10.061

6. Unnithan AR, Pichiah PBT, Gnanasekaran G, Seenivasan K, Barakat NAM, Cha YS, et al. Emu oil-based electrospun nanofibrous scaffolds for wound skin tissue engineering. Colloids and Surfaces A: Physicochemical and Engineering Aspects [Internet].

2012;415:454–60. Available from: http://dx.doi.org/10.1016/j.colsurfa.2012.09.029

7. Panawes S, Ekabutr P, Niamlang P, Pavasant P, Chuysinuan P, Supaphol P. Antimicrobial mangosteen extract infused alginate-coated gauze wound dressing. Journal of Drug Delivery Science and Technology [Internet]. 2017;41:182–90. Available from: https://doi.org/10.1016/j.jddst.2017.06.021

8. Croisier F, Jérôme C. Chitosan-based biomaterials for tissue engineering. European Polymer Journal [Internet]. 2013;49(4):780–92. Available from: http://dx.doi.org/10.1016/j.eurpolymj.2012.12.009

9. Zhang JF, Sun X. Mechanical properties of poly(lactic acid)/starch composites compatibilized by maleic anhydride. Biomacromolecules. 2004;5(4):1446–51.

10. Wang J, Sun B, Tian L, He X, Gao Q, Wu T, et al. Evaluation of the potential of rhTGF- β3 encapsulated P(LLA-CL)/collagen nanofibers for tracheal cartilage regeneration using mesenchymal stems cells derived from Wharton's jelly of human umbilical cord. Materials Science Engineering C [Internet]. 2017;70:637–45. Available from: http://dx.doi.org/10.1016/j.msec.2016.09.044

11. Silva SS, Popa EG, Gomes ME, Cerqueira M, Marques AP, Caridade SG, et al. An investigation of the potential application of chitosan/aloe-based membranes for regenerative medicine. Acta Biomaterialia [Internet]. 2013;9(6):6790–7. Available from: http://dx.doi.org/10.1016/j.actbio.2013.02.027

12. Silva SS, Caridade SG, Mano JF, Reis RL. Effect of crosslinking in chitosan/aloe vera-based membranes for biomedical applications. Carbohydrate Polymers [Internet]. 2013 Oct 15 [cited 2017 Sep 15];98(1):581–8. Available from: http://www.sciencedirect.com/science/article/pii/S0144861713006188?via%3Dihub

13. Van Nieuwenhove I, Salamon A, Peters K, Graulus GJ, Martins JC, Frankel D, et al. Gelatin- and starch-based hydrogels. Part A: Hydrogel development, characterization and coating. Carbohydrate Polymers [Internet]. 2016;152:129–39. Available from: http://dx.doi.org/10.1016/j.carbpol.2016.06.098

14. Noreen A, Nazli Z i. H, Akram J, Rasul I, Mansha A, Yaqoob N, et al. Pectins functionalized biomaterials; a new viable approach for biomedical applications: A review. International Journal of Biological Macromolecules [Internet]. 2017;101:254–72. Available from: http://dx.doi.org/10.1016/j.ijbiomac.2017.03.029

15. Ramanathan G, Singaravelu S, Muthukumar T, Thyagarajan S, Perumal PT, Sivagnanam UT. Design and characterization of 3D hybrid collagen matrixes as a dermal substitute in skin tissue engineering. Material Science and Engineering C [Internet]. 2017;72:359–70. Available from: http://dx.doi.org/10.1016/j.msec.2016.11.095

16. Capanema NSV, Mansur AAP, de Jesus AC, Carvalho SM, de Oliveira LC, Mansur HS. Superabsorbent crosslinked carboxymethyl cellulose-PEG hydrogels for potential wound dressing applications. International Journal of Biological Macromolecules [Internet]. 2018;106:1218–34. Available from: https://doi.org/10.1016/j.ijbiomac.2017.08.124

17. Yadav I, Rathnam VSS, Yogalakshmi Y, Chakraborty S, Banerjee I, Anis A, et al. Synthesis and characterization of polyvinyl alcohol- carboxymethyl tamarind gum based composite films. Carbohydrate Polymers [Internet]. 2017;165:159–68. Available from: http://dx.doi.org/10.1016/j.carbpol.2017.02.026

18. Li Y, Tan Y, Xu K, Lu C, Wang P. A biodegradable starch hydrogel synthesized via thiol-ene click chemistry. Polymer Degradation and Stability [Internet]. 2017;137:75–82. Available from: http://dx.doi.org/10.1016/j.polymdegradstab.2016.07.015

19. Nasri-Nasrabadi B, Mehrasa M, Rafienia M, Bonakdar S, Behzad T, Gavanji S. Porous starch/cellulose nanofibers composite prepared by salt leaching technique for tissue engineering. Carbohydrate Polymers [Internet]. 2014;108(1):232–8. Available from: http://dx.doi.org/10.1016/j.carbpol.2014.02.075

20. Kalia, Susheel, Avérous L. Biodegradable and Biobased Polymers for Environmental and Biomedical Applications [Internet]. 1st ed. Beverly,MA: Wiley; 2016. Available from: https://ebookcentral.proquest.com/lib/usfq/reader.action?docID=4386911

21. Zuo Y, Liu W, Xiao J, Zhao X, Zhu Y, Wu Y. Preparation and characterization of dialdehyde starch by one-step acid hydrolysis and oxidation. International Journal for Biological Macromolecules [Internet]. 2017;103:1257–64. Available from: http://dx.doi.org/10.1016/j.ijbiomac.2017.05.188

22. Zhang YR, Wang XL, Zhao GM, Wang YZ. Preparation and properties of oxidized starch with high degree of oxidation. Carbohydrate Polymers [Internet]. 2012;87(4):2554–62. Available from: http://dx.doi.org/10.1016/j.carbpol.2011.11.036

23. Zhang SD, Zhang YR, Wang XL, Wang YZ. High carbonyl content oxidized starch prepared by hydrogen peroxide and its thermoplastic application. Starch/Staerke. 2009;61(11):646–55.

24. Kyle Cetrulo, Curtis L. Cetrulo and RRT. Perinatal Stem Cells [Internet]. 2nd ed. Hoboken, NJ: Wiley; 2013. Available from: https://ebookcentral.proquest.com/lib/usfq/reader.action?docID=1124087

25. Anzalone R, Iacono M Lo, Loria T, Stefano A Di, Giannuzzi P, Farina F, et al. Wharton's Jelly Mesenchymal Stem Cells as Candidates for Beta Cells Regeneration: Extending the Differentiative and Immunomodulatory Benefits of Adult Mesenchymal Stem Cells for the Treatment of Type 1 Diabetes. Stem Cell Reviews and Reports. 2011;7(2):342–63.

26. Stoltz J. Regenerative Medicine and Cell Therapy [Internet]. Amsterdam: IOS Press; 2012. Available from: https://ebookcentral.proquest.com/lib/usfq/reader.action?docID=1137451

27. Elmi Sharlina MS, Yaacob WA, Lazim AM, Fazry S, Lim SJ, Abdullah S, et al. Physicochemical Properties of Starch from Dioscorea pyrifolia tubers. Food Chemistry [Internet]. 2017;220:225–32. Available from: http://dx.doi.org/10.1016/j.foodchem.2016.09.196

28. Smith RJ. Characterization and analysis of starches. Starch: Chemistry and Technology. 1967;620–625.

29. Parovuori P, Hamunen A, Forssell P, Autio K, Poutanen K. Oxidation of Potato Starch by Hydrogen Peroxide. Starch - Stärke. 1995;

30. Ellens CJ. Design, optimization and evaluation of a free-fall biomass fast pyrolysis reactor and its products. Graduate Theses Dissertations, Iowa State University. 2009;1–155.

31. Tanyildizi MS, Özer D, Elibol M. Optimization of α-amylase production by Bacillus sp. using response surface methodology. Process Biochemistry. 2005;40(7):2291–6.

32. Brown RC, Heindel TJ. Development of a lab-scale auger reactor for biomass fast pyrolysis and process optimization using response surface methodology. Graduate Theses Dissertations, Iowa State University. 2009;1-261.

33. Asfaram A, Ghaedi M, Hajati S, Goudarzi A, Bazrafshan AA. Simultaneous ultrasound-assisted ternary adsorption of dyes onto copper-doped zinc sulfide nanoparticles loaded on activated carbon: Optimization by response surface methodology. Spectrochimica Acta - Part A: Molar and Biomolecular Spectroscopy [Internet]. 2015;145:203–12. Available from: http://dx.doi.org/10.1016/j.saa.2015.03.006

34. Sigma-Aldrich. Technical Bulletin [Internet]. Available from: https://www.sigmaaldrich.com/content/dam/sigma-aldrich/docs/Sigma/Bulletin/b6916bul.pdf

35. Osundahunsi OF, Fagbemi TN, Kesselman E, Shimoni E. Comparison of the Physicochemical Properties and Pasting Characteristics of Flour and Starch from Red and White Sweet Potato Cultivars Comparison of the Physicochemical Properties and Pasting Characteristics of Flour and Starch from Red and White Sweet. Food Chemistry. 2003;1499:2232–6.

36. Hernández-Medina M, Torruco-Uco JG, Chel-Guerrero L, Betancur-Ancona D. Caracterización fisicoquímica de almidones de tubérculos cultivados en Yucatán, México. Ciência e Tecnologia de Alimentos [Internet]. 2008;28(3):718–26. Available from: http://www.scielo.br/pdf/cta/v28n3/a31v28n3.pdf

37. Lewandowski CM, Co-investigator N, Lewandowski CM. Starch Chemistry and Technology. 3rd Edition. Vol. 1, The effects of brief mindfulness intervention on acute pain experience: An examination of individual difference. 2015. 1689-1699 p.

38. Salmi T, Tolvanen P, Wärnå J, Mäki-Arvela P, Murzin D, Sorokin A. Mathematical modeling of starch oxidation by hydrogen peroxide in the presence of an iron catalyst complex. Chemical Engineering Science [Internet]. 2016;146:19–25. Available from: http://dx.doi.org/10.1016/j.ces.2016.02.027

39. Dias ARG, Zavareze EDR, Helbig E, Moura FA De, Vargas CG, Ciacco CF. Oxidation of fermented cassava starch using hydrogen peroxide. Carbohydrate Polymers [Internet]. 2011;86(1):185–91. Available from: http://dx.doi.org/10.1016/j.carbpol.2011.04.026

40. Sun F, Liu J, Liu X, Wang Y, Li K, Chang J, et al. Effect of the phytate and hydrogen peroxide chemical modifications on the physicochemical and functional properties of wheat starch. Food Research International [Internet]. 2017;100(January):180–92.

Available from: http://dx.doi.org/10.1016/j.foodres.2017.07.001

41. Steiner ET, Guthrie JD. Determination of Starch in Sweet Potato Products and Other Plant Materials. Industrial and Engineering Chemistry - Analytical Edition. 1944;16(12):736–9.

42. Verardi A, Blasi A, Marino T, Molino A, Calabrò V. Effect of steam-pretreatment combined with hydrogen peroxide on lignocellulosic agricultural wastes for bioethanol production: Analysis of derived sugars and other by-products. Journal of Energy Chemistry [Internet]. 2018;27(2):535–43. Available from: https://doi.org/10.1016/j.jechem.2017.11.007

43. Yu J, Chang PR, Ma X. The preparation and properties of dialdehyde starch and thermoplastic dialdehyde starch. Carbohydrate Polymers [Internet]. 2010;79(2):296–300. Available from: http://dx.doi.org/10.1016/j.carbpol.2009.08.005

44. Lyu Y, Ren H, Yu M, Li X, Li D, Mu C. Using oxidized amylose as carrier of linalool for the development of antibacterial wound dressing. Carbohydrate Polymers [Internet]. 2017;174:1095–105. Available from: http://dx.doi.org/10.1016/j.carbpol.2017.07.033

45. Silva R, Singh R, Sarker B, Papageorgiou DG, Juhasz-Bortuzzo JA, Roether JA, et al. Hydrogel matrices based on elastin and alginate for tissue engineering applications. International Journal of Biological Macromolecules. 2018;114:614–25.

46. Nourmohammadi J, Ghaee A, Liavali SH. Preparation and characterization of bioactive composite scaffolds from polycaprolactone nanofibers-chitosan-oxidized starch for bone regeneration. Vol. 138, Carbohydrate Polymers. 2016. p. 172–9.

47. Marie Arockianathan P, Sekar S, Kumaran B, Sastry TP. Preparation, characterization and evaluation of biocomposite films containing chitosan and sago starch impregnated with silver nanoparticles. International Journal of Biological Macromolecules [Internet]. 2012;50(4):939–46. Available from: http://dx.doi.org/10.1016/j.ijbiomac.2012.02.022

48. Moreno O, Cárdenas J, Atarés L, Chiralt A. Influence of starch oxidation on the functionality of starch-gelatin based active films. Carbohydrate Polymers. 2017;178(August):147–58.

49. Liu Y, Ma L, Gao C. Facile fabrication of the glutaraldehyde cross-linked collagen / chitosan porous scaffold for skin tissue engineering [Internet]. Vol. 32, Materials Science & Engineering C. 2012. p. 2361–6. Available from: http://dx.doi.org/10.1016/j.msec.2012.07.008

50. Li T, Song X, Weng C, Wang X, Sun L, Gong X, et al. Self-crosslinking and injectable chondroitin sulfate/pullulan hydrogel for cartilage tissue engineering. Vol. 10, Applied Materials Today. 2018. p. 173–83.

51. Zareidoost A, Yousefpour M, Ghaseme B, Amanzadeh A. The relationship of surface roughness and cell response of chemical surface modification of titanium. Journal of Materials Science: Materials in Medicine. 2012;23(6):1479–88.

52. Yamashita D, Machigashira M, Miyamoto M, Takeuchi H, Noguchi K, Izumi Y, et al. Effect of surface roughness on initial responses of osteoblast-like cells on two types of

zirconia. Dental Materials Journal. 2009;28(4):461–70.

53. Tang IM, Krishnamra N, Charoenphandhu N, Hoonsawat R, Pon-On W. Biomagnetic of apatite-coated cobalt ferrite: A core-shell particle for protein adsorption and pH-controlled release. Nanoscale Research Letters. 2012;7:1–10.

54. Li D, Ye Y, Li D, Li X, Mu C. Biological properties of dialdehyde carboxymethyl cellulose crosslinked gelatin – PEG composite hydrogel fibers for wound dressings. Carbohydrate Polymers. 2016;137:508–14.